JOURNAL OF MATERIALS SCIENCE 22 (1987) 612–616

Influences of grain size and precracking load on the critical stress intensity factor of mild steel

JI-LIANG DOONG, JIUN-REN HWANG, HSING-SHIH CHEN
Department of Mechanical Engineering, National Central University, Chung-li, Taiwan, Republic of China

The effects of grain size and precracking load on the critical stress intensity factor are studied. A plane stress model of elastic–plastic stress distribution which includes the strain hardening effects is used. The effects of residual stresses and strain hardening due to fatigue load are calculated by choosing plastic zone size as fracture criterion. Experimental results are obtained to demonstrate the reliability of theoretical calculations.

1. Introduction

In the test procedures for critical stress intensity factor measurements, it is recommended procedure to precrack the specimen by fatigue. But the possible effects of residual stresses caused by fatigue are not considered.

In order to establish the role played by residual stress distributions in crack propagation rates, several authors [1, 2] have attempted to calculate and measure the residual stresses by different models and experimental techniques. For example, Elber [3], and Adans [4] focused on crack closure phenomena to obtain information on residual stress. A direct measurement of residual stress performed in photoelastic materials is given in [5]. Tirosh [6] used a theoretical model, based on dislocation mechanics, to predict the residual stress distribution resulting from fatigue cracking. Dahl [7] has studied experimentally the influence of plastic zone size on fracture toughness.

It has been proven for many alloys, especially for the lower yield point of steels, that the grain size has an influence on the tensile yield stress. The lower yield stress of α-iron is often taken to depend on the inverse square root of the polycrystal ferrite grain diameter according to the Hall–Petch relation [8, 9],

$$\sigma_y = \sigma_{0y} + k_y d^{-1/2} \quad (1)$$

where σ_{0y} and k_y are experimental constants, d and σ_y are grain size and yield strength, respectively. Investigations have been made as to the influence of grain size on other mechanical properties such as fatigue properties [10, 11], crack propagation [12, 13] and fracture toughness [7, 14, 15]. It is not surprising perhaps, that the effect of grain size on K_{Ic} fracture toughness has not been clarified. All the above-mentioned papers focus on experimental results.

There are few papers which discuss the influence of precrack histories on fracture toughness. This is also true for theoretical analysis. The authors [16] used a plane stress model of elastic–plastic stress distribution to study the influences of residual stress and strain hardening on the critical stress intensity factors. The critical plastic zone is chosen as fracture criterion to evaluate the instability of crack extension. In the present paper, this work is extended to study the effect of grain size on the critical stress intensity factor during the different precracking loads. Hall–Petch effects are added to the previous computer program, and experimental results are obtained to show the reliability of theoretical calculations.

2. Stress distribution near a crack

The stress distribution in a cracked element can be calculated by the theory of elasticity, with the assumption of linear elastic behaviour.

The most simple model is an infinite sheet loaded by a tensile stress σ (Fig. 1). The Westergaard method [17] of calculating the stress distribution near a sharp crack is the best method to examine the properties of a particular type of crack. A suitable complex function is chosen to satisfy boundary conditions and the properties of compatability. The solution of plane stress distribution $S(x)$ in an infinite plate with a small crack length $2c$ under uniaxial tension at $y = 0$ is given as follows:

$$S(x) = \frac{\sigma}{[1 - (c/x)^2]^{1/2}} \quad (2)$$

The stress distribution of a plate with finite width $2b$ can be obtained by modifying the solution of a factor $f(c)$ which is derived by making the summation stresses equal to applied load. This characteristic is shown in Equations 3 and 4.

$$\sigma 2b = 2\int_c^b \sigma^* x(x^2 - c^2)^{-1/2}\,dx \quad (3)$$

$$\sigma^* = \sigma b(b^2 - c^2)^{-1/2} = \sigma f(c) \quad (4)$$

where $f(c) = b(b^2 - c^2)^{-1/2} = [1 - (c/b)^2]^{-1/2} = (1 - N^2)^{-1/2}$ in which the dimensionless parameter $N = c/b$ is used.

Analytical solutions of stress distribution in the field of a mixed elastic–plastic field has been obtained for a plane stress model. Considering the elastic stress distribution in plane stress, as shown in Fig. 2, the plastic zone is supposed to extend a distance $D_2 - c$ ahead of the crack tip ($x = c$). Owing to strain

0022–2461/87 $03.00 + .12

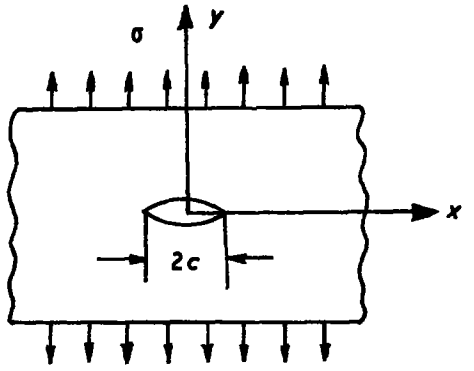

Figure 1 Westergaard's model of a crack under uniaxial tension in an infinite plate.

hardening, the tensile stress $S(x)$ is assumed to be linearly distributed beyond the yield strength within this zone. So $S(D_2) = \sigma_y$ and we define $S(c) = \sigma_c$. The material outside the plastic zone is assumed to be the same as the elastic stress. The elastic stress is distributed for an imaginary, extended crack of length $2c_1$, which is expressed by curve BC.

Lal [18] has studied the influence of ultimate strength σ_u on plastic tensile instability. It was proved that the area of yielded zone decreases as hardness of the material increases. He pointed out that as the stress at the crack tip exceeds the ultimate tensile strength of the material, the crack extends further through the plastically deformed region. For this reason, σ_c may be assumed equal to σ_u after fatigue cracking.

The stress distributions over the whole plate under loading condition are shown in Equations 5 and 6.

$$S(x) = (\sigma_c - \sigma_y)(D_2 - x)/(D_2 - c) + \sigma_y \qquad D_2 \geqslant x > c \tag{5}$$

$$S(x) = \sigma f(c_1) x(x^2 - c^2)^{-1/2} \qquad x \geqslant D_2 \tag{6}$$

and $S(D_2) = \sigma_y$,

$$\sigma_y = \sigma f(c_1) D(D_2^2 - c_1^2)^{-1/2} \tag{7}$$

The value of c_1 can be determined under the condition that the total loads or curve ABC and curve $A'B'C'$ are the same

$$\int_c^b S(x)\,dx = \int_c^b \sigma f(c) x(x^2 - c^2)^{-1/2}\,dx \tag{8}$$

$$\int_c^{D_2} S(x)\,dx + \int_{D_2}^b S(x)\,dx = \sigma f(c) \int_c^b x(x^2 - c^2)^{-1/2}\,dx \tag{9}$$

$$\tfrac{1}{2}(D_2 - c)(\sigma_y + \sigma_c) + \sigma f(c_1)(x^2 - c_1^2)^{-1/2}\Big|_{D_2}^b = \sigma f(c)(x^2 - c^2)^{-1/2}\Big|_c^b \tag{10}$$

$$\tfrac{1}{2}(D_2 - c)(\sigma_y + \sigma_c) - \sigma f(c_1)(D_2^2 - c_1^2)^{-1/2} = 0 \tag{11}$$

The two unknowns c_1 and D_2 can be obtained by solving Equations 7 and 11 simultaneously.

If the strip is unloaded, the stress in the plastic zone does not fit with the elastic stress distribution. This misfitting causes residual stresses. Full elastic unloading will cause residual compressive stresses at A exceeding the compressive yield strength. As a result of the unloading process, a reversed plastic deformation will occur between c and D_4. Obviously $D_4 - c$ is much smaller than $D_2 - c$. The elastic–plastic stress distribution $R(x)$ and plastic zone size after unloading are solved by the same procedure as loading condition. Compressive yield strength is assumed to be equal to tensile yield strength. Equations 12 and 13 are used to solve c_2 and D_4

$$-\sigma_y = \frac{D_2 - D_4}{D_2 - c}(\sigma_c - \sigma_y) + \sigma_y - \sigma f(c_2) D_4/(D_4^2 - c_2^2)^{-1/2} \tag{12}$$

$$(\sigma_c + \sigma_y)(D_4 - c) + \tfrac{1}{2}(D_4 - c)\frac{D_2 - D_4}{D_2 - c}(\sigma_c - \sigma_y) - \sigma f(c)(D_4^2 - c^2)^{-1/2} = \sigma f(c_2)(D_4^2 - c_2^2)^{-1/2} \tag{13}$$

It can be seen that c_2 and D_4 are found by simultaneously solving Equations 12 and 13. If the strain

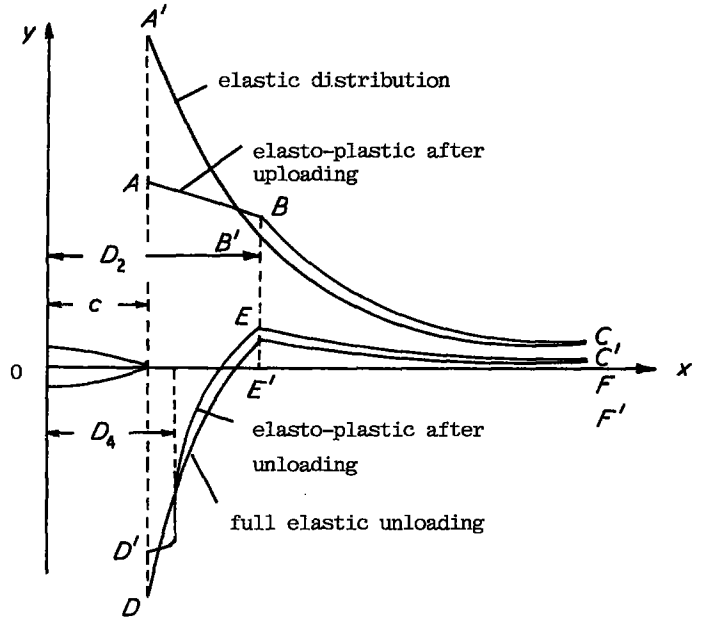

Figure 2 Schematic elastic–plastic stress distribution near a notch after loading and unloading.

TABLE I Chemical composition of the steel investigated in wt %

Element	C	Si	Mn	P	S	Cr	Ni	Cu
wt %	0.0758	0.0934	0.2859	0.0037	0.034	0.0417	0.0311	0.111

hardening effect does not exist, then the material within the plastic zone is rigid–perfectly plastic and σ_c is equal to yield strength σ_y.

3. Experimental procedure and results

Chemical compositions of the plain carbon steel specimen are given in Table I. A range of grain size from 1.19 to 6.03 μm in diameter was provided by heat treatments at various temperatures for various times as shown in Table II. The material was machined to the centre crack specimens as shown in Fig. 3, by electric discharge machining. The specimens were pre-cracked to $\sim$18.5 mm under three different load conditions . The method of measuring the K_c values is suggested [19] on a closed loop electro-hydraulic testing machine at room temperature. The K_c value can be calculated by the following equation [20]

$$K_c = \frac{P}{t}\left[\frac{\pi\alpha}{2W}\sec\left(\frac{\pi\alpha}{2}\right)\right]^{-1/2} \quad (14)$$

where P is a fracture load and t is specimen thickness. $\alpha = 2a/W$ and $W = 2b$. The results of yield strength σ_y and K_c values are shown in Table IV. From the experimental data, the constants σ_{0y} and k_y in Equation 1 can be obtained by the least square method. These data are listed in Table III.

4. The influence of fatigue load on fracture behaviour

There are two reasons for the influence of fatigue load on critical stress intensity values. Before our discussion, we should choose a suitable fracture criterion, critical plastic zone ϱ_{cr}, to prevent instability crack extension from occurring. Fracture philosophy by means of plastic zone size is similar to the COD (crack opening displacement) concept, but has the advantage that the plastic zone is easily determined by K-value cancellation of the Dugdale crack model [21], and it is convenient to calculate the effects of strain hardening and compressive residual stress on K_c from this criterion directly. It is well known that under plastic deformation when strained to a particular value of the stress, say σ^*_{yp} (see Fig. 4) a number of dislocation sources are activated, as a result of which the dislocation density increases. The resistance to further deformation also increases. When the material is released and reloaded, yielding of the material does not take place until the value of the applied stress reaches the value of σ^*_{yp}. In other words, the yield strength of the strained material is increased to σ^*_{yp}. This effect can be evaluated by Equation 15.

$$\text{Strain hardening effect} = \int_c^{c+\varrho_{cr}} [\sigma^*_{yp}(x) - \sigma_y]\,dx \quad (15)$$

The second reason is compressive residual stresses. Dahl [7] had studied the influence of plastic zone size on the fracture toughness value. He concluded that fracture toughness increased with plastic zone size. Within plastic zone size the compressive residual stresses are the main reason to increase the critical stress intensity factor.

The residual stresses between the crack tip and $c + \varrho_{cr}$ can affect the load P in Equation 14. Compressive residual stress must be compensated by external load which makes the fracture load P increase. Conversely, tensile residual stress has an inverse effect on fracture load. This effect is equal to

$$\text{Residual stresses effect} = \int_c^{c+\varrho_{cr}} R(x)\,dx \quad (16)$$

where $R(x)$ is elastic plastic stress distribution after unloading.

For theoretical calculation, critical plastic zone must be determined first. Burdekin [22] using the Dugdale method has derived Equation 17

$$\delta = \frac{8\sigma_y a}{\pi E}\log\sec\frac{\pi\sigma}{2\sigma_y} = \frac{8\sigma_y a}{\pi E}\left[\frac{1}{2}\left(\frac{\pi}{2}\frac{\sigma}{\sigma_y}\right)^2 + \frac{1}{12}\left(\frac{\pi}{2}\frac{\sigma}{\sigma_y}\right)^4 + \cdots\right] \quad (17)$$

for nominal stress value less than $0.75\sigma_y$, a reasonable approximation for δ (crack opening displacement),

TABLE II Grain diameter and heat treatment condition

d(μm)	Heat treatment condition
1.19	900° C 0.5 h, furnace cooling to 700° C, then air cooling
3.01	1000° C 1 h, furnace cooling to 700° C, then air cooling
4.64	1000° C 2 h, furnace cooling to 700° C, then air cooling
6.03	1100° C 5 h, furnace cooling to 700° C, then air cooling

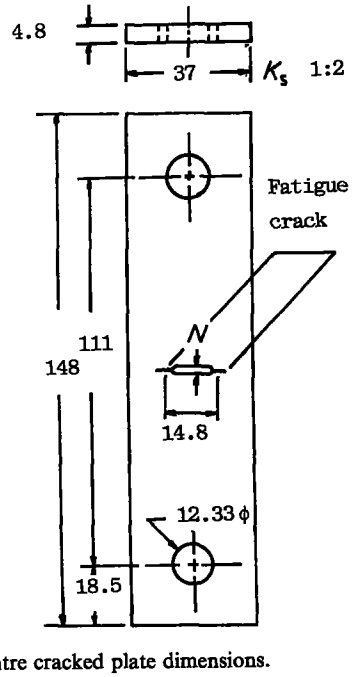

Figure 3 Centre cracked plate dimensions.

TABLE III Yield strength and ultimate strength of different grain size specimen

$d(\mu m)$	1.19	3.01	4.64	6.03
$\sigma_y(kg\,mm^{-2})$	35.96	31.66	31.10	30.63
$\sigma_u(kg\,mm^{-2})$	45.59	45.80	48.85	53.64

Note: the constants of σ_{0y} and k_y are equal to 25.61 and 0.35.

using only the first term of this series is

$$\delta = \frac{\pi\sigma^2 a}{E\sigma_y} \tag{18}$$

For a through-thickness crack of length $2a$,

$$K_I = \sigma\sqrt{\pi a} \tag{19}$$

thus,

$$\delta E\sigma_y = K_I^2 \tag{20}$$

Since $E = \sigma_y/\varepsilon_y$, the following relation exists:

$$\frac{\delta}{\varepsilon_y} = \left(\frac{K_I}{\sigma_y}\right)^2 \tag{21}$$

Substituting Equation 18 into Equation 19 eliminates σ. At the onset of crack instability, we can get

$$\frac{\delta_{cr}}{\varepsilon_y} = \left(\frac{K_c}{\sigma_y}\right)^2 \tag{22}$$

From the Dugdale approach

$$\frac{a}{a+\varrho} = \cos\frac{\pi\sigma}{2\sigma_y} = 1 - \frac{1}{2!}\left(\frac{\pi\sigma}{2\sigma_y}\right)^2 + \frac{1}{4!}\left(\frac{\pi\sigma}{2\sigma_y}\right)^4 - \cdots \tag{23}$$

Neglecting higher order term, ϱ is found as

$$\varrho = \frac{\pi^2\sigma^2 a}{8\sigma_y^2} = \frac{\pi K_I^2}{8\sigma_y^2} \tag{24}$$

By substituting Equation 20 into Equation 24, and at the onset

$$\varrho_{cr} = \frac{\pi E}{8\sigma_y}\delta_{cr} \tag{25}$$

Equation 25 is identical with the limit form of ϱ for $\sigma/\sigma_y \to 0$ on the basis of the Dugdale model, and its general applicability, irrespective of σ/σ_y value, have been verified experimentally [21]. For the material used in our studies, modified value of K_c (mod) is

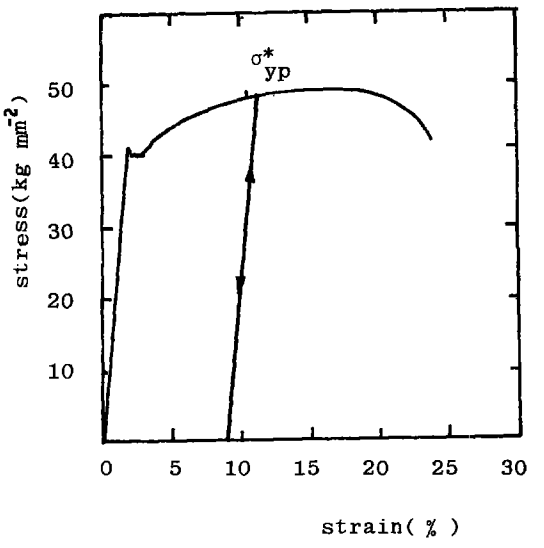

Figure 4 Stress–strain curve.

calculated by iteration and shown in Table IV. The parameters A and B are

$$A = 2t\int_c^{c+\varrho_{cr}} [\sigma_{yp}^*(x) - \sigma_y]\,dx$$

$$B = -2t\int_c^{c+\varrho_{cr}} R(x)\,dx$$

And $P_a = P_{ex} - A - B$ where P_{ex} is the experimental fracture load. P_a is the true fracture load which is subtracted $A + B$ from P_{ex}. $A + B$ expresses the double effects of strain hardening and compressive residual stresses. In Table IV, a very interesting behaviour can be seen. K_c (exp) values which were calculated by P_{ex} are increased with the increasing of grain size. It conflicts with the Hall–Petch effect, but the values K_c (mod) modified by the present computer program agree with the Hall–Petch effect. From Table III, the differences between yield strength and ultimate strength increased with the increasing of grain size. Thus it can be concluded that strain hardening effects are dominant for larger grain size (also shown in Table IV and compared to the values of A). Modified results K_c (mod) in which both strain hardening and residual stresses effects are considered are compared with experimental results in Table IV. From these results, it can be seen that the percentage errors of $(P_a - P_{av})/P_{av} \times 100\%$ are significantly lower than experimental values $(P_{ex} - P_{av})/P_{av} \times 100\%$. The predicted data of K_c (theo) which are calculated from Hall–Petch relationship and computer program directly are shown in Table IV. It can be seen that

TABLE IV Experimental, modified and theoretical results

$d(\mu m)$	M	$2c$ (mm)	P_{ex} (kg)	K_c (exp) ($kg\,mm^{-3/2}$)	A(kg)	B(kg)	P_a(kg)	K_c (mod) ($kg\,mm^{-3/2}$)	K_c (theo) ($kg\,mm^{-3/2}$)
1.19	0.244	19.61	3150	136.69	154.31	4.06	2988.6	131.33	131.25
	0.365	18.64	3400	139.41	160.21	14.82	3216.3	132.83	132.76
	0.487	19.50	3550	142.25	165.79	41.85	3300.5	133.06	132.99
3.01	0.244	19.12	3600	137.88	310.90	2.69	3283.8	126.59	126.95
	0.365	17.10	4075	138.00	316.17	9.82	3739.2	127.66	127.98
	0.487	17.94	3575	138.24	291.14	22.42	3239.2	125.28	125.62
4.64	0.244	20.73	3475	141.10	370.01	2.35	3100.3	126.16	125.90
	0.365	18.30	3775	138.17	368.76	9.12	3388.3	124.01	123.92
	0.487	19.36	3550	139.44	360.76	17.40	3154.4	123.90	124.20

theoretically predicted data concisely matched with modified data. It is shown that the present model is suitable to calculate the effect of precrack load on critical stress intensity factor measurement. The effects of grain size can be included in the present computer program, and true K_c values can be obtained under arbitrary fatigue loading conditions.

5. Conclusion

A study is made on the influences of grain size under different precracking loads on the critical stress intensity factor under plane stress condition. The results obtained are summarized as follows:

1. Analytical results are closely matched with the experimental data.

2. Hall–Petch effects can be included in the present computer program for mild steels. K_c values increased with the decreasing of grain sizes.

3. The effect of precracking load on the K_c value can be explained through the strain hardening effect and compressive residual stress within the plastic zone size.

4. The true K_c value can be obtained by subtracting the combined load differences due to strain hardening and compressive residual stress from the experimental result under arbitrary fatigue loading conditions.

References

1. M. L. WILLIAM, *J. Appl. Mech.* **79** (1957) 108.
2. G. R. IRWIN, *ibid.* **82** (1960) 417.
3. W. ELBER, *Eng. Fracture Mech.* **2** (1970) 37.
4. N. J. I. ADAMS, *ibid.* **4** (1972) 543.
5. P. S. THEOCARIS and E. E. GDOUTOS, *ibid.* **7** (1975) 331.
6. J. TIROSH and A. LADELSKI, *ibid.* **12** (1980) 453.
7. W. DAHL and W. B. KRETZSCHMANN, in Proceedings of the Fourth International Conference on Fracture, Waterloo, Canada, June 1977 edited by D. M. R. Taplin (Pergamon Press, New York, 1978) pp. 17–21.
8. E. O. HALL, *Proc. Phys. Soc. (Lond.)* **(64)B** (1951) 747.
9. N. J. PETCH, *J. Iron Steel Inst. (Lond.)* **173** (1953) 25.
10. A. W. THOMPSON and W. A. BACKOFEN, *Acta Met.* **19** (1971) 597.
11. L. P. KARJALAINEN, *Scripta Met.* **7** (1973) 43.
12. R. R. SEELEY, MSc thesis, Youngstown State University, 1974.
13. F. R. STONESIFER and R. W. ARMSTRONG, *Eng. Fracture Mech.* **10** (1978) 305.
14. *Idem,* in Proceedings of the Fourth International Conference on Fracture, Waterloo, Canada, June 1977 edited by D. M. R. Taplin (Pergamon Press, New York, 1978) pp. 1–6.
15. S. K. CHAUDHURI and R. BROOK, *Int. J. Fracture* **12** (1976) 101.
16. H. S. CHEN and J. L. DOONG, *J. Mater. Sci.* **18** (1983) 2305.
17. H. M. WESTERGAARD, *J. Appl. Mech.* **61** (1939) A49.
18. K. M. LAL, *Trans. ASME, JEMT* (1975) 84.
19. E. S. JOHN and F. B. WILLIAM, *ASTM STP* **381** (American Society for Testing and Materials, Philadelphia, 1965) 133.
20. C. E. FEDDERSEN, *ibid.* **410** (1976) 77.
21. F. KOSHIGA, in "Significance of Defects in Welded Structures" (University of Tokyo Press, Tokyo, 1973) pp. 283–91.
22. F. M. BURBEKIN and D. E. W. STONE, *J. Strain Anal.* **1** (1966) 145.

Received 24 February
and accepted 22 May 1986